Strong measurement and quantum feedback for persistent Rabi oscillations in circuit QED experiments

Mazyar Mirrahimi Benjamin Huard Michel Devoret

Abstract— We consider the stabilization of the dynamical state of a superconducting qubit. In a series of papers, A. Korotkov and his co-workers suggested that continuous weak measurement of the state of a qubit and applying an appropriate feedback on the amplitude of a Rabi drive, should allow maintaining the coherence of the Rabi oscillations on an infinite horizon. Here, in the aim of approaching a metrological application of these persistent Rabi oscillations, we study a new variant of such strategies based on performing strong measurements in a discrete-in-time manner and applying the measurement record to correct the phase of the Rabi oscillations. Noting that, such persistent Rabi oscillations can be seen as an amplitude-to-frequency convertor (converting the amplitude of the Rabi micro-wave drive to a precise frequency), we propose another feedback layer (consisting of a simple analog phase locked loop) to compensate the low frequency deviations in the amplitude of the Rabi drive.

I. INTRODUCTION

Recent advances on superconducting qubits have led to lifetimes and coherence times of several microseconds [11], [6]. In parallel, the advances on quantum-limited Josephson parametric amplifiers [16], [1], [12] have made it possible to measure continuously the state of a qubit without adding mostly classical noise. Indeed, Quantum Non-Demolition (QND) measurement of a superconducting qubit coupled to a microwave resonator through a Josephson parametric amplifier has been recently achieved in the experiment of [17]. All these advances open the doors to invest real-time quantum feedback schemes for preparing and protecting various quantum states of interest in quantum information or metrology [14].

In a series of papers [13], [18], [9], A. Korotkov and co-workers proposed feedback strategies to stabilize the coherent oscillations in a qubit when driven by a resonant Rabi drive. While an important difficulty in the initial scheme [13] was the necessity to solve in real-time a Bayesian filter equation, in a second scheme, Korotkov proposed a simple analog scheme to stabilize the Rabi oscillations [9].

This stabilization problem can have a very important metrological application. Indeed, the Rabi oscillations of a qubit can be seen as an amplitude-to-frequency convertor,

converting the amplitude of the resonant drive to the frequency of the induced Rabi oscillations. Therefore, a high-precision measurement of this frequency leads to a high-precision measurement of the microwave drive's amplitude allowing the stabilization of the microwave generator's output power. However, due to the dephasing of the qubit, these oscillations admit very short lifetimes and are rapidly invaded by phase noise. This is why compensating this dephasing in a feedback procedure is very important.

Here, in the aim of addressing this metrological application, we propose a new closed-loop phase correction scheme that maintains with an acceptable fidelity the phase of the coherent oscillations and furthermore allows for a correction of the low-frequency deviations in the Rabi drive amplitude. The main idea consists in correcting the phase of the coherent oscillations in a discrete-in-time manner and during the time between two corrections to accumulate information on the amplitude of the Rabi drive. Indeed, similarly to [5], we propose to perform strong qubit measurements at every half period of the desired Rabi oscillation. The phase error can then be corrected by applying π-pulses each time we observe the opposite phase to the one expected. A second feedback layer, based on the output of a continuous weak measurement of the qubit, allows for correcting the deviations in the Rabi drive amplitude and stabilizing it around some nominal value.

Throughout this paper, we will perform simulations by considering the parameters that should be quite easily achievable in experiments with charge qubits such as transmons. Also, while the second feedback layer consists of a simple analog phase locked loop, the first one can be implemented in a real-time experiment using present digital electronics like Field Programmable Gate Array boards.

In the next section, we will start with a brief introduction to the circuit QED model and the dispersive measurement of the qubit. Also, we will show how, through a quantum Zeno effect, discrete-in-time strong measurements can enhance the coherence of the Rabi oscillations. Finally, we will show how a simple feedback scheme based on the output of these measurements and corrective π-pulses can lead to persistent Rabi oscillations. In Section III, we will add the second feedback layer and we will show how a simple Phase Locked Loop based on the output of a continuous weak measurement, can stabilize the Rabi drive amplitude against low frequency deviations.
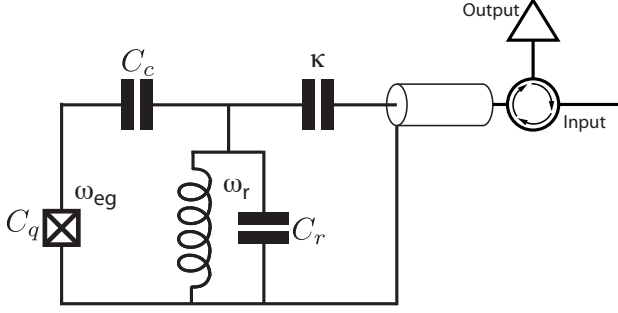
Fig. 1. Scheme of the transmon qubit coupled to a superconducting resonator with strength $g = \sqrt{\omega_r \omega_{eg}} \frac{C_c}{2\sqrt{C_r(C_c+C_q)}}$ (see e.g. [3]). The qubit state can be manipulated and read out dispersively using microwave fields sent to the input port and measured at the output port of the amplifier.

II. DISCRETE-TIME STRONG MEASUREMENT AND FEEDBACK

A. Circuit QED model

We consider here a quantum circuit consisting of a transmon qubit [7] of transition frequency ω_{eg} coupled to a superconducting resonator of frequency ω_r (see the scheme of Fig. II-A). We further assume this coupling to be in the dispersive regime, meaning that the coupling strength is smaller than the detuning between the resonator and qubit frequencies. Driving the resonator at its resonance frequency by microwave signals, the effective Hamiltonian after a rotating wave approximation is given as follows:

$$H_{\text{eff}} = \hbar \frac{\omega_{eg}}{2}\sigma_z + \hbar\chi a^\dagger a \sigma_z + \hbar[\epsilon_d(t)a^\dagger + \epsilon_d^*(t)a]. \quad (1)$$

Here a is the field annihilation operator, and $\sigma_z = |e\rangle\langle e| - |g\rangle\langle g|$ is the Pauli operator in qubit space and ϵ_d is the complex amplitude of the microwave drive at frequency ω_r. Finally, χ is the dispersive coupling strength given by $\chi = \alpha g^2/\Delta(\Delta + \alpha)$ [7] where α is the anharmonicity of the transmon qubit defined as $\alpha = \omega_{fe} - \omega_{eg}$ (ω_{fe} being the transition frequency between the first and second excited states), g is the coupling strength between the qubit and resonator (see Fig. II-A) and $\Delta = \omega_{eg} - \omega_r$. Indeed, we are in the regime where $|\Delta| \gg g$ (in fact, we even assume that $|\Delta| \gg 2g\sqrt{\bar{n}}$ where $\bar{n}$ is the average number of photons in the resonator).

B. Dispersive measurement and reduced master equation

In the Born-Markov approximation, the Lindblad master equation describing the evolution of the density matrix of the coupled qubit-resonator is given by [2], [10]

$$\frac{d}{dt}\rho_t = -\frac{i}{\hbar}[H_{\text{eff}}, \rho_t]$$
$$+ \kappa\mathcal{D}[a]\rho_t + \gamma_1\mathcal{D}[\sigma_-]\rho_t + \gamma_\phi\mathcal{D}[\sigma_z]\rho_t/2, \quad (2)$$

where κ is the resonator's decay rate (through its coupling to the transmission line), γ_1 is the qubit decay rate, γ_ϕ the pure

dephasing rate, $\sigma_- = |g\rangle\langle e|$ is the qubit lowering operator and $\mathcal{D}[A]$ the damping superoperator

$$\mathcal{D}[A]\rho = A\rho A^\dagger - A^\dagger A\rho/2 - \rho A^\dagger A/2.$$

Starting with a state of the form $|g\rangle \otimes |0\rangle$ (resp. $|e\rangle \otimes |0\rangle$) where $|0\rangle$ is the vacuum state of the associated resonator's mode, and neglecting the energy loss due to γ_1 (in practice $\gamma_1 \ll \kappa$ allows to decouple adiabatically the qubit dynamics from the resonator), the state at time t is given by $|g\rangle \otimes |\alpha_g(t)\rangle$ (resp. $|e\rangle \otimes |\alpha_e(t)\rangle$) where $|\alpha_{g(e)}(t)\rangle$ are coherent states of the resonator with complex amplitudes determined by

$$\frac{d}{dt}\alpha_g(t) = -i\epsilon_d(t) - (\kappa/2 - i\chi)\alpha_g(t)$$
$$\frac{d}{dt}\alpha_e(t) = -i\epsilon_d(t) - (\kappa/2 + i\chi)\alpha_e(t)$$
$$\alpha_g(0) = \alpha_e(0) = 0. \quad (3)$$

In this work, we are interested in measurement scenarios where the measurement drive is turned on with a constant (rather strong) amplitude $\epsilon_d(t) \equiv \bar{\epsilon}_d \in \mathbb{R}$ on a short time interval (comparable to the resonators decay time κ^{-1}). If the drive is turned on during a time τ only, the coherent states α_g and α_e are given by (see Fig. 2)

$$\alpha_g(t) = -\frac{2i\bar{\epsilon}_d}{\kappa - 2i\chi}\left(1 - e^{-\frac{(\kappa-2i\chi)}{2}t}\right) \qquad t \in [0, \tau],$$

$$\alpha_g(t) = \frac{2i\bar{\epsilon}_d e^{-\frac{(\kappa-2i\chi)}{2}t}}{\kappa - 2i\chi}\left(1 - e^{\frac{(\kappa-2i\chi)}{2}\tau}\right) \qquad t > \tau,$$

$$\alpha_e(t) = -\alpha_g^*(t).$$

These coherent states act as pointer states for the qubit. Detection of the in-phase quadrature amplitude $I = \langle a + a^\dagger\rangle/2$ allows us to distinguish between these two coherent states and thus readout the state of the qubit. Following the derivation of Ref. [4], one finds the laboratory frame reduced qubit master equation

$$\frac{d}{dt}\rho_t = -i\frac{\omega_{\text{ac}}(t)}{2}[\sigma_z, \rho_t]$$
$$+ \gamma_1\mathcal{D}[\sigma_-]\rho_t + (\gamma_\phi + \gamma_m(t))\mathcal{D}[\sigma_z]\rho_t/2. \quad (4)$$

Here,

$$\gamma_m(t) = 2\chi\text{Im}(\alpha_g(t)\alpha_e^*(t)) = -2\chi\text{Im}(\alpha_g(t)^2),$$

is an additional dephasing due to the coupling to the populated resonator and

$$\omega_{\text{ac}}(t) = \omega_{eg} + B(t),$$

with $B(t) = 2\chi\text{Re}(\alpha_g(t)\alpha_e^*(t)) = -2\chi\text{Re}(\alpha_g(t)^2)$ the ac-stark shift experimentally measured in Ref. [15].

C. Measurement record and quantum Zeno effect

As discussed above, the average effect of the measurement procedure can lead to additional dephasing. Furthermore, this dephasing rate γ_m increases with $\bar{\epsilon}_d$ in a quadratic way. Therefore, stronger measurements should increase dramatically the dephasing. However, we will see through this
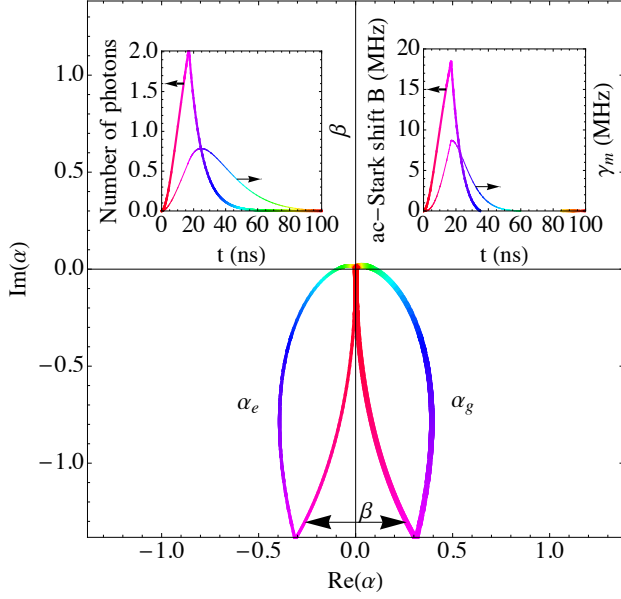
Fig. 2. Evolution of the field state in the resonator when the drive $\bar{\epsilon}_d/2\pi = 22$ MHz is turned on for 17 ns and is then turned off. The cavity pull is chosen to be $\chi/2\pi = 5$ MHz and the cavity decay rate $\kappa/2\pi = 20$ MHz. The main plot represents the evolution of the two possible field states α_g and α_e over 100 ns in the quadrature space, the time being color coded. The corresponding photon number $|\alpha|^2$ and distance between possible fields β are plotted on the top left inset. The additional dephasing $\gamma_m(t)$ due to the coupling to the resonator, and the ac-stark shift $B(t)$ are shown in the top right inset. It can be seen that the atom-resonator coupling is negligible after 50 ns which is the measurement duration in the proposed experiment.

subsection that discrete strong measurements at half-periods of Rabi oscillations sharpen the noise power peak at Rabi frequency.

The measurement record observed in an experiment can be expressed as

$$J_t = \sqrt{\kappa}\beta(t)\,\langle\sigma_z\rangle_t + \frac{1}{\sqrt{\eta}}\xi_t \qquad (5)$$

where ξ_t is a Gaussian white noise which represents the photon shot noise and the separation between field state is

$$\beta(t) = |\alpha_g(t) - \alpha_e(t)|. \qquad (6)$$

Let us consider Rabi oscillations of frequency Ω_R. Starting from the excited state $|e\rangle$ (corresponding to $Z = 1$ for the Bloch sphere coordinates) at time $t = 0$, we know that in the absence of any dephasing and relaxation, the trajectories should pass by $Z = 1$ at times $\frac{2k\pi}{\Omega_R}$ and by $Z = -1$ at times $\frac{(2k+1)\pi}{\Omega_R}$. Similarly to [5], we consider the situation where the measurement is performed in a discrete manner and on short time intervals centered around the times where the qubit is supposed to pass by these two poles ($Z = \pm 1$).

Indeed, assuming a resonator's bandwidth much larger than the Rabi oscillations frequency ($\kappa \gg \Omega_R$), we perform the measurement by integrating the output amplitude (5) on the time intervals $\mathcal{I}_k = [\frac{k\pi}{\Omega_R} - \frac{\pi}{\kappa}, \frac{k\pi}{\Omega_R} + \frac{\pi}{\kappa}]$, of length $2\pi/\kappa$ and centered around the desired Rabi peaks $\frac{k\pi}{\Omega_R}$. The probe drive is turned on during the first third of these interval $\mathcal{I}_k$ only. The last two thirds of this interval are needed by the

resonator to relax to its vacuum state. The integrated output over this interval is then given by

$$J_k = \sqrt{\kappa}\int_0^{2\pi/\kappa} \beta(t)\,\langle\sigma_z\rangle_{\left(t + \frac{k\pi}{\Omega_R} - \frac{\pi}{\kappa}\right)}\, dt + W(\frac{2\pi}{\eta\kappa}), \quad (7)$$

where $\eta \leq 1$ is the efficiency of the measurement and $W(2\pi/\eta\kappa)$ is a Gaussian random variable with zero mean and standard deviation $\sqrt{2\pi/\eta\kappa}$.

We consider this discrete output signal as a discretization of a continuous signal with time steps of length π/Ω_R. Applying a Discrete Fourier Transform, we can therefore compute the power spectral density corresponding to this signal. Let us analyze the effect of the strength of the measurement on this spectrum through some simulations.
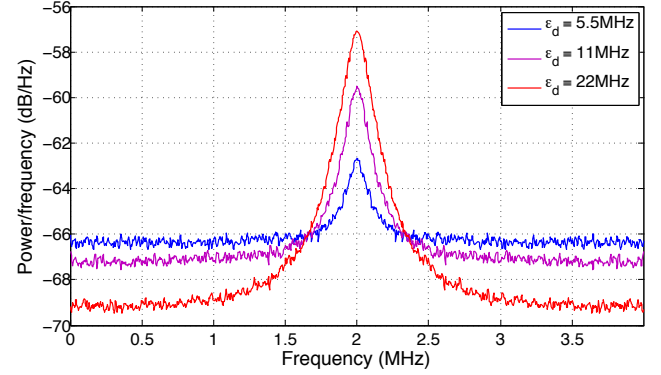

Fig. 3. Power spectral density for the discrete measurement record; taking respectively $\bar{\epsilon}_d/2\pi = 5.5, 11, 22$ MHz

Here we take the parameters $\Omega_R/2\pi = 2$ MHz, $\kappa/2\pi = 20$ MHz, $\chi/2\pi = 5$ MHz, $\eta = 1$, $\gamma_1/2\pi = .05$ MHz and $\gamma_\phi/2\pi = .1$ MHz, corresponding to $T_1 = 3.18$ μs and $T_2 = 1.27$ μs (see Remarks 2.1 and 2.3 for some details on the choice of parameters). The simulations of Figure 3 then illustrate the power spectral density of the recorded discrete signal over 1 ms for $\epsilon_d/2\pi$ ranging from 5.5 to 22 MHz. We observe a net increase of the peak around 2 MHz (Rabi frequency) with the increase of the measurement strength. Indeed, by quantum Zeno effect, simply reading out the qubit state refocuses the qubit to the nearest pole of the Bloch sphere with a good probability, hence overcoming the dephasing of the qubit to some extent. However, relaxation events can induce a phase inversion of the Rabi oscillations. As it will be seen in the next subsection correcting these phase inversions with a simple feedback based on the result of this discrete measurement lead to a narrow peak in the power spectral density at frequency Ω_R.

Remark 2.1: The considered qubit relaxation and dephasing times can easily be achieved for instance with transmons in compact resonators. We choose each measurement duration to be 50 ns which is a small part of the 250 ns between two measurements. Choosing a longer measurement duration would disturb the Rabi oscillations of the qubit by freezing it along the Z-axis. In order to ensure a measurement duration as short as 50 ns, we need the resonator's bandwidth to be as large as 20 MHz. Indeed, we need such a decay rate for the resonator to ensure that we are able to entangle the

resonator to the qubit, readout the resonator and let them get un-entangled through the resonator's decay to vacuum, within these 50 ns. Moreover, the bandwidth κ does not need to be larger than the one of the first amplifier. Here, we set $\kappa/2\pi = 20$ MHz.

D. Bayesian filter and feedback

In this subsection, based on the above measurement scheme, we propose a simple feedback strategy allowing to compensate the dephasing of the qubit and to maintain the coherence of the Rabi oscillations.

Let us start by providing a simple filter equation that allows us to estimate the state of the qubit, based on the integrated measurement outcomes J_k. Let us take the state of the qubit (in the Bloch sphere coordinates) after the k'th measurement to be (X_k, Y_k, Z_k). In order, to estimate the state after the measurement $k+1$ we proceed as follows. The state just before the measurement $k + 1$ can be estimated by

$$\begin{pmatrix} X^-_{k+1} \\ Y^-_{k+1} \\ Z^-_{k+1} \end{pmatrix} = S(\frac{\pi}{\Omega_R}, 0) \begin{pmatrix} X_k \\ Y_k \\ Z_k \end{pmatrix} - \gamma_1 \begin{pmatrix} C_x \\ C_y \\ C_z \end{pmatrix}, \qquad (8)$$

where $S(t_1, t_2)$ is a 3 by 3 matrix, solution of the equation

$$\frac{\partial}{\partial t_1} S(t_1, t_2) = \begin{pmatrix} -\gamma_2(t) & -\omega_{ac} & 0 \\ \omega_{ac} & -\gamma_2(t) & \Omega_R \\ 0 & -\Omega_R & -\gamma_1 \end{pmatrix} S(t_1, t_2),$$

$$\frac{\partial}{\partial t_2} S(t_1, t_2) = -\frac{\partial}{\partial t_1} S(t_1, t_2),$$

$$S(t, t) = \mathbb{1},$$

with $\gamma_2(t) = \gamma_m(t) + \gamma_\phi + \frac{\gamma_1}{2}$ and

$$\begin{pmatrix} C_x \\ C_y \\ C_z \end{pmatrix} = \int_0^{\frac{\pi}{\Omega}} S(\frac{\pi}{\Omega_R}, t) \begin{pmatrix} 0 \\ 0 \\ 1 \end{pmatrix} dt.$$

Indeed, since between two measurements we do not include any information update from the measurement outputs, the dynamics of the qubit is simply given by the reduced master equation (4) where the Rabi oscillations of frequency Ω_R around the X-axis are further added.

Following, a similar analysis to [8], the state of the qubit after the measurement number $k + 1$ can be updated as follows:

$$X_{k+1} = \frac{2e^{-\frac{\eta\kappa J^2_{k+1}}{4\pi}} e^{-\frac{\kappa(2-\eta)\mathcal{J}^2}{4\pi}} X^-_{k+1}}{(1+Z^-_{k+1})e^{-\frac{\eta\kappa(J_{k+1}-\mathcal{J})^2}{4\pi}} + (1-Z^-_{k+1})e^{-\frac{\eta\kappa(J_{k+1}+\mathcal{J})^2}{4\pi}}}$$

$$Y_{k+1} = \frac{2e^{-\frac{\eta\kappa J^2_{k+1}}{4\pi}} e^{-\frac{\kappa(2-\eta)\mathcal{J}^2}{4\pi}} Y^-_{k+1}}{(1+Z^-_{k+1})e^{-\frac{\eta\kappa(J_{k+1}-\mathcal{J})^2}{4\pi}} + (1-Z^-_{k+1})e^{-\frac{\eta\kappa(J_{k+1}+\mathcal{J})^2}{4\pi}}}$$

$$Z_{k+1} = \frac{(1+Z^-_{k+1})e^{-\frac{\eta\kappa(J_{k+1}-\mathcal{J})^2}{4\pi}} - (1-Z^-_{k+1})e^{-\frac{\eta\kappa(J_{k+1}+\mathcal{J})^2}{4\pi}}}{(1+Z^-_{k+1})e^{-\frac{\eta\kappa(J_{k+1}-\mathcal{J})^2}{4\pi}} + (1-Z^-_{k+1})e^{-\frac{\eta\kappa(J_{k+1}+\mathcal{J})^2}{4\pi}}},$$

(9)

where

$$\mathcal{J} = \int_0^{2\pi/\kappa} \sqrt{\kappa}\beta(t)dt.$$

Remark 2.2: In the strong measurement limit, we can approximate the above conditional dynamics by $X_{k+1} = Y_{k+1} = 0$ and Z_{k+1} as provided. Indeed, in this limit, we can approximate our measurement as an imperfect projective measurement. Through the following simulations, we will apply this simplified filter.

Now, based on the state of the quantum filter at step k, we consider the simple feedback consisting in a π-pulse around the X-axis as soon as we observe the opposite phase to the one we were expecting. Indeed, having started from $Z = 1$ at $t = 0$, we expect to have $Z_k \approx -1$ (resp. $Z_k \approx 1$) for k odd (resp. k even). Then, the feedback consists in applying a π-pulse as soon as we observe $Z_k > 0$ for k odd or $Z_k < 0$ for k even.

Applying such a feedback algorithm to the discretely measured qubit with the same parameters as in the previous subsection, one finds the power spectral density of Figure 4. The feedback leads to a δ-peak at the measurement frequency (here the same as the Rabi frequency).

Remark 2.3: The considered qubit relaxation and dephasing times are much longer than the typical delays achievable using present digital electronics like Field Programmable Gate Array boards. The proposed total feedback loop could realistically take between 70 and 200ns using this technology. In these simulations we have considered a feedback delay of 100 ns (i.e. the possible corrective π-pulses are applied 100 ns after performing the strong measurement). Furthermore, we fix the desired Rabi frequency around $\Omega_R/2\pi = 2$ MHz. This would give us about 250 ns between two measurements which seems to be enough to perform the computations of the quantum filter (8)-(9) and therefore to decide whether we need or not to apply a π-pulse. Note that, trying to stabilize Rabi oscillations that are much slower than this would decrease the final fidelity being defined as the degree of coherence which will be conserved. Indeed, by decreasing the Rabi frequency, or equivalently by increasing the interval between two measurements, we loose the control over the decoherence through this passive period.
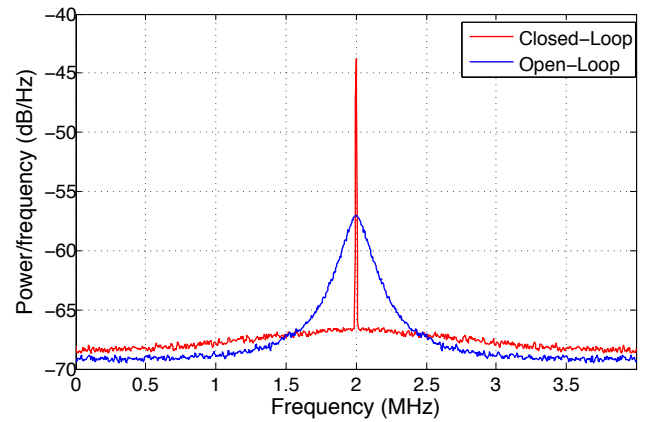

Fig. 4. Power spectral density for the strong measurement record ($\bar{\epsilon}_d/2\pi = 22$ MHz); the blue curve corresponds to the open-loop case while the red curve illustrates the effect of feedback.

We will see in Section III how such Rabi oscillations whose frequency are fixed by the measurement frequency
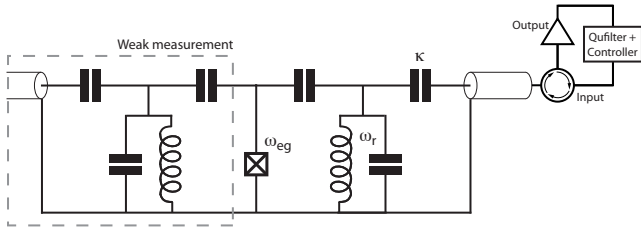
Fig. 5. Scheme of considered setup. The transmon qubit is coupled to two superconducting resonators. The qubit state can be controlled using a strong measurement feedback loop connected to the right resonator. The feedback corrected Rabi oscillations can then be observed independently using the left cavity, in the weak measurement regime.
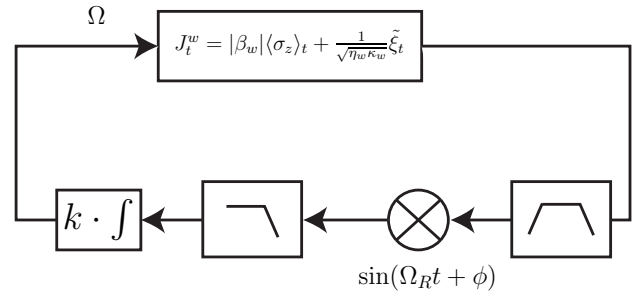

Fig. 6. The basic phase-locked loop allowing to lock the phase of the Rabi oscillations and therefore stabilizing the Rabi drive amplitude. The weak measurement output signal is first band-pass filtered, then modulated at the desired Rabi frequency Ω_R with a possible added phase. The resulting signal is low-pass filtered and integrated with a gain k before being sent to the microwave source as a power setpoint.

can be used to correct the low frequency deviations in driving RF power.

III. TOWARDS A ROBUST SOURCE OF DRIVING POWER

In the aim of stabilizing a desired Rabi oscillation of frequency Ω_R, we perform the strong measurements with a period of π/Ω_R and we apply corrective π-pulses if necessary. However, the drive amplitude at the input of the resonator might deviate from the value corresponding to the Rabi frequency Ω_R on time scales that are much larger than the qubit's coherence time. Typically, temperature variations lead to a few percent variations in the emitted power of a commercial source generator. Furthermore, microwave setups in cryogenic environment can also add some power fluctuations. This deviation will imply a small dephasing in the Rabi oscillation of the qubit between two strong measurements. In order to measure this dephasing and compensate it by stabilizing the microwave drive, we consider a second measurement through a second resonator which is also dispersively coupled to the qubit but is weakly and constantly driven (Fig. 5).

The measurement record is given by

$$ J_t^w = \sqrt{\kappa_w}\beta_w\langle\sigma_z\rangle_t + \frac{1}{\sqrt{\eta_w}}\tilde{\xi}_t, \qquad (10) $$

where κ_w is the bandwidth of the second resonator, β_w is defined as in (6) but for the coherent field of the second resonator, η_w is the detection efficiency of the weak measurement process and the Gaussian white noise $\tilde{\xi}_t$ is assumed to be independent from ξ_t in (5). Moreover, as we assume the resonator to be constantly driven in time, we can restrict ourselves to the steady-state solution of (3) and therefore β_w is constant in time.

A. Phase-locked loop and Rabi frequency synchronization

Here, we propose a feedback scheme, based on the continuous weak measurement record, allowing to control the drive amplitude and therefore, to lock the phase of the Rabi oscillations. The Figure 6 illustrates the diagram of such a phase locked loop. This loop consists in a multiplication of the output record (after a bandpass filter centered at the desired Rabi frequency) with a sinusoid of desired frequency Ω_R and a phase which is chosen to be the same as the one

applied for the strong measurement (in practice we need to calibrate this phase to overcome the phase shift created by the non-symmetricity of the strong measurement, see Figure 2, and the delay in the feedback). The result passes then through a low-pass filter (with a bandwidth much smaller than the desired Rabi frequency) and finally is integrated to provide the new drive amplitude to be applied.

The Figure 7 illustrates an overall diagram of the proposed feedback scheme. A first feedback loop acting on the qubit and correcting its dephasing by corrective π-pulses is incorporated within a second feedback loop correcting (on a much longer time-scale) the Rabi drive amplitude.
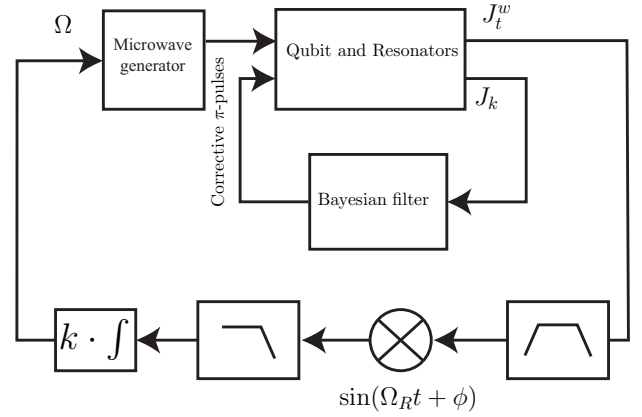

Fig. 7. Discrete strong measurements J_k are applied to correct the dephasing of the qubit with corrective π-pulses; a second loop acting at a much longer time-scale uses a continuous weak measurement record $J^w(t)$ to correct the deviations in the Rabi drive amplitude.

B. Simulations

The simulations of Figure 8 illustrate 10 runs of the above phase-locked loop to stabilize the Rabi drive amplitude (and therefore its induced Rabi frequency Ω). Having fixed the period of the strong measurements to 250 ns, we apply to the weak measurement signal a third order Butterworth bandpass filter centered at 2 MHz and with a bandwidth of 1 MHz. The filtered signal is then multiplied by a local oscillator of frequency 2 MHz with a calibrated phase and

the resulting signal is sent through a third order Butterworth low-pass filter with a cut-off frequency of 100 kHz. Finally, the result is integrated with an integration gain of $k/2\pi = 10$ Hz. We observe the stabilization of the induced Rabi frequency Ω (with a precision of about 10 kHz) around 2 MHz. This synchronization algorithm can even be used for slowly varying power setpoints.
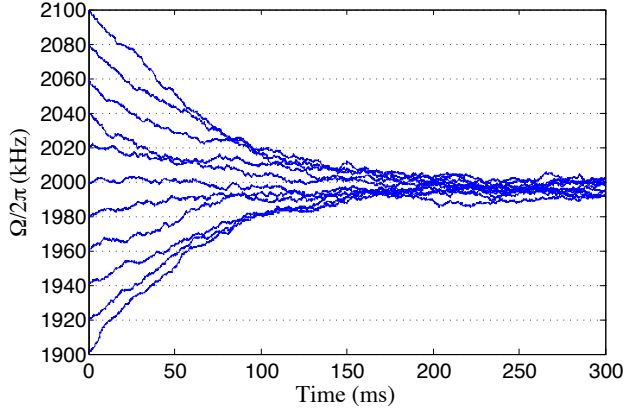

Fig. 8. Stabilization of the Rabi drive amplitude (and therefore its induced Rabi frequency Ω) around the frequency given by the strong measurement's period (here 250ns). Taking the qubit decay rates of $\gamma_1/2\pi = 50$ kHz and $\gamma_\phi/2\pi = 100$ kHz, the parameters $\kappa/2\pi = 20$ MHz, $\chi/2\pi = 5$ MHz, $\bar{\epsilon}_d/2\pi = 22$ MHz and $\eta = 1$ for the strong measurement, weak measurement parameters given by $\kappa_w/2\pi = 20$MHz, $|\beta_w| = .2$ and $\eta_w = 1$ and a feedback delay of 100 ns for corrective π-pulses, we ensure the convergence of Ω towards 2000 ± 5kHz.

IV. CONCLUSION

We have proposed a simple feedback scheme allowing to maintain coherent oscillations of a qubit. By applying corrective π-pulses based on the outcome of discrete-in-time strong measurements, we can correct the phase diffusion of the Rabi oscillations. Then the output of a second continuous weak measurement is applied in a second feedback layer to compensate the deviations in the amplitude of the Rabi micro-wave drive and to stabilize it around some nominal value given by the frequency of the strong measurements. While the second feedback layer is a simple analog phase locked loop the first one can be implemented in a real-time experiment using present digital electronics like Field Programmable Gate Array boards. Simulations based on realistic experimental parameters illustrate the performance of the proposed method.

REFERENCES

[1] B. Abdo, F. Schackert, M. Hatridge, C. Rigetti, and M.H. Devoret. Josephson amplifier for qubit readout. *Appl. Phys. Lett.*, 99:162506, 2011.

[2] H. Carmichael. *An Open Systems Approach to Quantum Optics*. Springer-Verlag, 1993.

[3] M. H. Devoret. Quantum fluctuations in electrical circuits. *Les Houches Session LXIII, Quantum Fluctuations*, pages 351–386, 1995.

[4] J. Gambetta, A. Blais, M. Boissonneault, A. A. Houck, D. I. Schuster, and S. M. Girvin. Quantum trajectory approach to circuit qed: Quantum jumps and the zeno effect. *Phys. Rev. A*, 77:012112, 2008.

[5] A. N. Jordan and M. Buttiker. Quantum nondemolition measurement of a kicked qubit. *Phys. Rev. B*, 71:125333, 2005.

[6] Z. Kim, B. Suri, V. Zaretskey, S. Novikov, K. D. Osborn, A. Mizel, F.C. Wellstood, and B.S. Palmer. Decoupling a cooper-pair box to enhance the lifetime to 0.2 ms. *Phys. Rev. Lett.*, 106:120501, 2011.

[7] J. Koch, T.M. Yu, J. Gambetta, A.A. Houck, D.I. Schuster, J. Majer, A. Blais, M.H. Devoret, S.M. Girvin, and R.J. Schoelkopf. Charge-insensitive qubit design derived from the cooper pair box. *Phys. Rev. A*, 76:042319, 2007.

[8] A.N. Korotkov. Continuous quantum measurement of a double dot. *Phys. Rev. B*, 60(8), 1999.

[9] A.N. Korotkov. Simple quantum feedback of a solid-state qubit. *Phys. Rev. B*, 71:201305, 2005.

[10] G. Lindblad. On the generators of quantum dynamical semigroups. *Communications in Mathematical Physics*, 48:119–30, 1976.

[11] H. Paik, D.I. Schuster, L.S. Bishop, G. Kirchmair, G. Catelani, A.P. Sears, B.R. Johnson, M.J. Reagor, L. Frunzio, L.I. Glazman, S.M. Girvin, M.H. Devoret, and R.J. Schoelkopf. Observation of high coherence in josephson junction qubits measured in a three-dimensional circuit qed architecture. *Phys. Rev. Lett.*, 107:240501, 2011.

[12] N. Roch, E. Flurin, F. Nguyen, P. Morn, P. Campagne-Ibarcq, M. H. Devoret, and B. Huard. Widely tunable, non-degenerate three-wave mixing microwave device operating near the quantum limit. *Phys. Rev. Lett.* To be published.

[13] R. Ruskov and A.N. Korotkov. Quantum feedback control of a solid-state qubit. *Phys. Rev. B*, 66:041401, 2002.

[14] C. Sayrin, I. Dotsenko, X. Zhou, B. Peaudecerf, T. Rybarczyk, S. Gleyzes, P. Rouchon, M. Mirrahimi, H. Amini, M. Brune, J.-M. Raimond, and S. Haroche. Real-time quantum feedback prepares and stabilizes photon number states. *Nature*, 477:73–77, 2011.

[15] D. I. Schuster, A. Wallraff, A. Blais, L. Frunzio, R.-S. Huang, J. Majer, S. M. Girvin, and R. J. Schoelkopf. ac stark shift and dephasing of a superconducting qubit strongly coupled to a cavity field. *Phys. Rev. Lett.*, 94:123602, 2005.

[16] R. Vijay, M.H. Devoret, and I. Siddiqi. Invited review article: The Josephson bifurcation amplifier. *Rev. Sci. Instrum.*, 80:111101, 2009.

[17] R. Vijay, D. H. Slichter, and I. Siddiqi. Observation of quantum jumps in a superconducting artificial atom. *Phys. Rev. Lett.*, 106:110502, 2011.

[18] Q. Zhang, R. Ruskov, and A.N. Korotkov. Continuous quantum feedback of coherent oscillations in a solid-state qubit. *Phys. Rev. B*, 72:245322, 2005.